Refractive power of a multilayer rotationally symmetric model of the human cornea and tear film

Sergio Barbero

School of Optometry, Indiana University, Bloomington, Indiana, 47405

Received September 20, 2005; revised December 22, 2005; accepted January 24, 2006; posted February 7, 2006 (Doc. ID 64881)

Optical models of the human cornea and tear film typically employ a single homogeneous cornea with an average refractive index. I propose to use a more realistic multilayer model based on morphological data from the literature. The mathematical methodology to derive the refractive power equation of this model is presented. Special attention is given to the axial gradient index of the refraction structure of the stroma layer because of its optical implications. The importance of considering this multilayer model is quantified in a specific example (orthokeratology) with the help of the derived power equation. © 2006 Optical Society of America

OCIS codes: 330.5370, 080.2730, 080.2710.

1. INTRODUCTION

The human cornea and tear film provide most of the refractive power of the eye. Hence, a classical problem in visual optics is to estimate their refractive power. Historically, two optical models have been used: a single-surface model and a single-lens (two surfaces) model. Both models assume spherical surfaces (or conic surfaces in some schematic models[1]) and an average refractive index for the cornea and tear film. Such models are used with the hope of being sufficiently accurate for most practical purposes. However, much more is now known about the internal structure and optical properties of the cornea than when these models were originally proposed. Further, actual clinical practice has to deal with many situations where the internal structure (in optical terms) of the cornea is modified: for example, corneal pathologies or refractive correction techniques such as orthokeratology or refractive surgery. Clearly, the uniform single-lens models cannot predict the internal optical power changes in these situations, whereas a multilayer model can estimate whether these internal changes are relevant for the optical power. The main goal of this work is to employ a multilayer rotationally symmetric model of the human cornea and tear film and to derive an equation of the corneal refractive power as a function of all the available parameters: curvature, asphericity, thickness, and refractive index distributions of the different layers—tear film, epithelium, and "extended stroma" (stroma and endothelium). The extended stroma is modeled with a gradient refractive index distribution. Pupil diameter and object position are also incorporated into this model. It will be shown how the power equation of this model generates valuable information about the contributions of the different optical components to the overall power of the cornea.

The paper is organized as follows. Section 2 describes the morphological model for the cornea and tear film. On the one hand, the model emphasizes the optical multilayer structure of the cornea. On the other hand, surfaces are assumed to be rotationally symmetric, described by conics, in order to present a generic model. The model is based strictly on optical properties determined experimentally and available from literature. Section 3 discusses the concept of plane of best focus. In Section 4 an algebraic expression for the paraxial power of the multilayer model is derived, and in Section 5 the formulas for the spherical aberration are added. Section 6 gives a specific example of the application of the new model for orthokeratology. Finally, Section 7 presents some discussion of the results and conclusions.

2. OPTICAL MODEL OF THE CORNEA AND TEAR FILM

The cornea and tear film constitute a multilayer structure in which the refractive index and the shape of the surfaces change across layers. Although higher irregularities and astigmatism are presented in corneal surfaces (at least in the outer surface), these are so variable among eyes that to model generic surfaces, it is reasonable to use conics. Indeed, the conic model of ocular surfaces is the one used in the ocular biometry literature. To avoid confusion in the notation, I employ the conic explicit formula $Y^2=2Rz-(1+Q)z^2$, where R is the apical radius and Q is the asphericity (or deformation factor). Q is the most convenient parameter to define optical surfaces because (see Section 5) it separates the asphericity from the spherical contribution in the spherical aberration formulas. To study the refraction properties in biological tissues it is necessary to use a locally averaged refractive index.[2] This issue will be specifically discussed for the stroma.

A. Optical Structure of the Tear Film

The traditional three layer model of the tear film structure (lipid, aqueous, and mucus layer) has been superseded by a more complex structure,[3] in which the transition between the mucus and aqueous layers is now

 © 2006 Optical Society of America

represented by a gradual transition from an aqueous dominated medium at the lipid border to a mucus-dominated medium at the epithelial border. This gradual biochemical transition is optically consistent with a gradient refractive index distribution because the refractive index of the mucus is higher than that of the aqueous-dominated medium. However, although the tear film may actually have a gradient index distribution, it can be represented by a homogeneous unique layer because it is only a few micrometers thick, and therefore the internal optical power (transfer) contribution is very small compared with the surface power contributions (see Table 2 below). I take 1.337 as a reference value, measured by Craig *et al.*[4] with a critical-angle refractometer (589 nm). There is great diversity in the values of tear film thickness in the literature, so I adopt the value of 4 μm as a possible average.

B. Corneal Optical Structure

The classical morphological model of the cornea is composed of five layers: epithelium, Bowman's membrane, lamellar stroma, Descemet's membrane, and endothelium. However, in terms of refractive index distribution, it is reasonable to model the last four layers as a unique layer with a gradient refractive index. This has been proposed by Patel *et al.*[5] and is justified below.

1. Thickness and Refractive Index

The epithelium is a highly stratified tissue formed by five to seven cell layers.[6] Patel *et al.*[5] report an average value of the epithelial layer thickness of 53.7 μm. In a previous work Patel *et al.*[7] measured the refractive index (Abbé refractometer D line) in ten subjects, finding an average value of 1.401 (ranging from 1.39 to 1.408).

The stroma is a connective tissue formed by a highly regular arrangement of parallel strings of fibrous proteins (collagen fibrils) embedded in a polysaccharide gel[8] (extracellular matrix). Bowman's and Descemet's layers are junction tissues for the stroma with similar structure, both very thin (8–12 μm[6]). The variation in refractive index between the collagen fibrils and the extrafibrillar matrix is spatially small scale, as the typical diameter of a collagen fibril is ~30 nm in diameter,[8] hence being responsible only for scattering effects. Refraction is modeled using a locally averaged refractive index that changes in large scale. Maurice[9] proposed a model in which the changes of the local refractive index in the stroma are due to two factors: the differences in the relative volume between collagen and extracellular matrix and the variations in the refractive index of the extracellular matrix. These factors change because of the biochemical differentiation between the anterior part (hydratation and glucose) and the posterior part of the stroma—a fact that has been known for some time.[7] This observation has been confirmed by Patel *et al.*,[7] who measured a difference in refractive index in six eyes (Abbé refractometer D line) from 1.380±0.005 in the anterior part to 1.373±0.001 in the posterior part. Considering this, it is reasonable to assume a smooth and linear variation of the refractive index in an extended-stroma model (Bowman's and Descement's layers included). The gradient refractive distribution is along the normal to the stroma surface layer. However, since the radius of curvature of the surface is much larger than the thickness of the stroma, it is a good approximation to assume that the transverse variation of the refractive index is negligible and therefore to assume a pure axial gradient. The endothelium is a single cell layer 5 μm,[8] where no refractive index information is available. However, because it is so thin, it is reasonable to integrate it into the extended-stroma model. Finally, I use the thickness for the extended stroma reported by Patel *et al.*[5] Figure 1 is a graphical visualization of the variation of the refractive index along the optical axis coordinate in the proposed model.

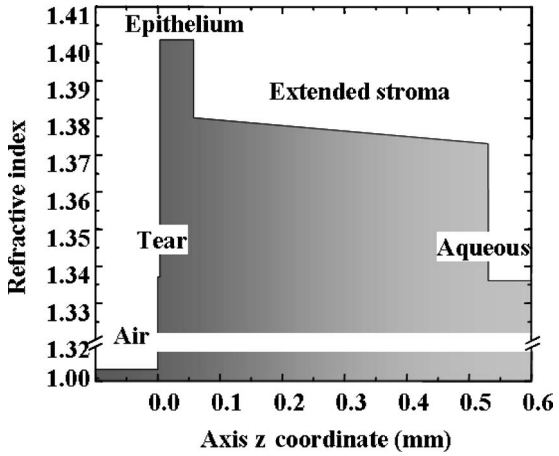

Fig. 1. Refractive index along the optical axis coordinate (in millimeters) in the cornea model. The *y* axis of the graphic is broken from 1.02 to 1.32 for better visualization.

2. Surface Modeling

The surfaces of the model are represented by conics. For the anterior and posterior corneal surfaces I use the measurements made by Dubbelman *et al.*[10] (who used a Scheimpflug slit lamp); they found an average radius for the anterior corneal surface of 7.87±0.27 mm and 6.40±0.28 mm for the posterior surface (83 subjects, ranging in age from 16 to 62 yr). The *Q* value of the anterior and the posterior corneal surfaces were −0.18±0.18 and −0.38±0.27, respectively.

The tear film is attached to the epithelium predominantly by surface tension; because of this, and with lack of experimental information, it is reasonable to assume that the tear film, in normal conditions, is uniformly distributed in the effective optical zone. Therefore, the shape of the air–tear-film interface is almost identical to that of tear-film–epithelium interface, the slight difference being due only to the effect of the thickness on the radius.

The epithelium of the cornea has been found to have a nonuniform thickness, being significantly thicker at the periphery than in the center (53.7 μm in the center and 56.2 μm at 1.5 mm from the center).[5] Using these data of the thickness distribution and the conic shape of the tear-film–epithelium interface, we obtain for the least-squares fitting of the epithelium–stroma interface to a conic a radius of 7.64 mm and asphericity of −1.55.

Table 1 summarizes the whole multilayer optical model used henceforth.

Table 1. Parameters of the Cornea and Tear-Film Multilayer Model

	Interface			
	Air–Tear	Tear–Epithelium	Epithelium–Stroma	Stroma–Aqueous
Radius (mm)	7.87[10]	7.87	7.64	6.4[10]
Q	−0.18[10]	−0.18	−1.55	−0.38[10]
	Medium			
	Tear	Epithelium	Stroma	Aqueous
Central thickness (mm)	0.004	0.0537[5]	0.473[5]	—
Refractive index	1.337[4]	1.401[7]	$\Delta n = 1.380 - 1.373$[7]	1.336

3. PLANE OF BEST FOCUS

It is reasonable to define an optical axis for the cornea and tear film shared by the different layers in normal conditions, although in some pathologies a single axis may not exist. With an optical axis and conic surfaces, a paraxial power of the cornea and tear can be evaluated (see Section 4). The conic model will manifest defocus and spherical aberration when one considers only on-axis objects; extension to off-axis objects would add odd aberrations. In addition, avoiding astigmatism simplifies the final algebraic expression significantly, since rotational symmetry reduces the number of parameters needed to describe the paraxial properties per surface to three (2×2 matrix).[11]

From wave aberrations, several objective metrics (usually correlated with visual performance) have been proposed to define the optical quality in the human eye—see, e.g., Cheng *et al.*[12] and references there. Considering that the model includes only the cornea, I reduce the number of available metrics for defining the plane of best focus to a pure optical metric. In the presence of significant aberrations (in this model, spherical aberration), diffraction phenomena have little effect on focus location.[13] Thus, for convenience, I use a metric based only on geometrical optics; moreover, the consideration of diffraction integrals would disable the derivation of a simple algebraic expression.

With all these considerations, the plane of best focus can be defined as the plane that minimizes the radius of gyration of the ray spot diagram, i.e., the sum of the squares of the distances of the ray spots to the optical axis.[14] Using this metric, we can derive a formula to obtain the plane of best focus[15]:

$$f = f_{\text{parax}} - \frac{2\sigma_1 \rho^2}{3v'}. \tag{1}$$

Here f is the distance of the plane of best focus from the principal plane, f_{parax} is the paraxial focal length, σ_1 is the transverse-ray spherical aberration, v' is the paraxial marginal-ray angle in the exit pupil of the cornea, and ρ is the radius of the exit pupil. To compute this formula it is necessary to derive equations for the paraxial focal length and the spherical aberration.

Finally, I should note that, for simplicity, I restrict the analysis to monochromatic light; an extension to polychromatic light would imply knowing the dispersion relations of the different media in the cornea and tear film.[16]

4. PARAXIAL OPTICS OF THE CORNEA AND TEAR FILM

A. Paraxial Optics

Considering the cornea as a centered system with an optical axis (z coordinate), ray propagation can be defined by two variables: the intersection point coordinate of the ray with a plane normal to the z axis (Y variable) and the angle of the ray vector with the z axis in that point (U variable). The cornea acts as an imaging system. Mathematically this implies that there is a mapping: $Y_1 = f(Y_0, U_0)$ and $U_1 = f(Y_0, U_0)$ relating the coordinates of the of the ray in the object plane (Y_0, U_0) and the coordinates of the same ray in the image plane (Y_1, U_1). Moreover, in paraxial optics $[\sin(U) \sim U]$ this mapping is linear. In matrix representation,

$$\begin{bmatrix} Y_1 \\ U_1 \end{bmatrix} = \begin{bmatrix} A & B \\ C & D \end{bmatrix} \begin{bmatrix} Y_0 \\ U_0 \end{bmatrix}, \tag{2}$$

where $ABCD$ is called the ray-transfer matrix and its elements (paraxial coefficients) depend on the parameters of the system,[17,18] i.e., curvatures, thickness, and refractive indices. For basic operations, such as translation in a homogeneous medium $\mathcal{T}$ and the refraction in a surface $\mathcal{R}$, the ray matrices are well known:

$$\mathcal{T} = \begin{bmatrix} 1 & t \\ 0 & 1 \end{bmatrix}, \qquad \mathcal{R} = \begin{bmatrix} 1 & 0 \\ -\mathcal{P}/n' & n/n' \end{bmatrix}. \tag{3}$$

Here t is the distance of propagation along the z coordinate, n and n' are the refractive indices in the first and second medium, respectively, and $\mathcal{P}$ is the refractive power in the surface defined as $\mathcal{P} = (n' - n)/R$ (R is the apical radius of the interface surface). An important property in paraxial optics is that sequential applications of ray-transfer transformations are equivalent to a unique matrix transformation calculated as the sequential multiplication of the individual ray-transfer matrices.[13] In addition, once the equivalent $ABCD$ matrix of the system is obtained, the cardinal points are straightforward to evaluate. The paraxial power is evaluated as $\mathcal{P} = -n'C$.

B. Ray-Transfer Matrix of the Cornea and Tear Film

With a single surface or homogeneous lens corneal model, the above formalism leads to the well-known paraxial formulas of the thick lens (which go back in time to Huygens's work[19]). However, in the present model the formula is more complex. First of all, the paraxial coefficients of the ray transfer inside the axial gradient index of the stroma have to be calculated. A concise derivation starting with the mixed characteristic Hamilton function can be found in Lunenburg's book.[17] Starting with the Euler–Lagrange ray equation, a fragmented derivation was given by Buchdahl,[18] followed by Sands.[20] For completeness, a detail derivation of the ray-transfer matrix for an axial gradient index, starting from the stationary action principle, is presented in Appendix A. Using translation, refraction, and axial ray transfer matrices, the global ray matrix for the cornea and tear film is

$$\begin{bmatrix} A & B \\ C & D \end{bmatrix} = \begin{bmatrix} 1 & 0 \\ -\mathcal{P}_4/n_4 & n_{32}/n_4 \end{bmatrix} \begin{bmatrix} 1 & \dfrac{t_3 n_{31} \ln(n_{32}/n_{31})}{(n_{31}-n_{31})} \\ 0 & n_{31}/n_{32} \end{bmatrix} \begin{bmatrix} 1 & 0 \\ -\mathcal{P}_3/n_{31} & n_2/n_{31} \end{bmatrix} \begin{bmatrix} 1 & t_2 \\ 0 & 1 \end{bmatrix} \begin{bmatrix} 1 & 0 \\ -\mathcal{P}_2/n_2 & n_1/n_2 \end{bmatrix} \begin{bmatrix} 1 & t_1 \\ 0 & 1 \end{bmatrix} \begin{bmatrix} 1 & 0 \\ -\mathcal{P}_1/n_1 & 1/n_1 \end{bmatrix}, \tag{4}$$

where $\mathcal{P}_1$, $\mathcal{P}_2$, $\mathcal{P}_3$, and $\mathcal{P}_4$ are the paraxial surface refractive powers in the interfaces: air–tear film, tear-film–epithelium, epithelium–anterior stroma, and posterior-stroma–aqueous humor, respectively; t_1, t_2, t_3 are the thickness of the tear film, epithelium, and extended stroma, respectively; and $n_1, n_2, n_{31}, n_{32}, n_4$ are the refractive indices of the tear film, epithelium, anterior stroma, posterior stroma, and aqueous humor, respectively. In addition, for comparison, I use a homogeneous refractive index for the stroma equal to $n_3 = 1.3765$. This value is obtained, using the so-called Gladstone and Dale law (proposed for the cornea by Maurice[9]), as the mean refractive index equivalent to that of the axial stroma model. From Eq. (4) and using $\mathcal{P} = -n'C$, we can derive the formula for the paraxial power. This is easily done with symbolic software (the code written in MATLAB is available from the author).

C. Paraxial Refractive Power of the Cornea and Tear Film

It is convenient to express the final algebraic expression for the paraxial power in expanded form to reveal the relative contributions of the layers of the model:

$$P = \sum_{i=1}^{4} P_i - \sum_{i=1}^{3} T_i + T_g, \tag{5}$$

where P_i is the interface refractive power between two attached layers, T_i is the individual transfer contribution inside a layer, and T_g is a global transfer contribution that, as we will see, can be practically neglected. The formulas for T_1, T_2, T_3 and T_g are as follows:

Both homogeneous and gradient stroma

$$T_1 = \frac{t_1(P_2 + P_3 + P_4)}{n_1}, \qquad T_2 = \frac{t_2(P_1 + P_2)(P_3 + P_4)}{n_2};$$

Homogeneous stroma

$$T_3 = \frac{t_3(P_1 + P_2 + P_3)}{n_3}$$

$$T_g = \frac{t_1 t_2 P_1 P_2 (P_3 + P_4)}{n_1 n_2} + \frac{t_2 t_3 P_3 P_4 (P_1 + P_2)}{n_2 n_3} + \frac{t_1 t_3 P_1 P_4 (P_2 + P_3)}{n_1 n_3} - \frac{t_1 t_2 t_3 P_1 P_2 P_3 P_4}{n_1 n_2 n_3},$$

Gradient stroma

$$T_3 = \frac{t_{31}(P_1 + P_2 + P_3)\log(n_{32}/n_{31})}{n_{31}(n_{32} - n_{31})}$$

$$T_g = \frac{\log(n_{32}/n_{31})}{n_{32} - n_{31}} \left(\frac{t_1 t_2 P_1 P_2 (P_3 + P_4)}{n_1 n_2} + \frac{t_2 t_3 P_3 P_4 (P_1 + P_2)}{n_2 n_3} + \frac{t_1 t_3 P_1 P_4 (P_2 + P_3)}{n_1 n_3} - \frac{t_1 t_2 t_3 P_1 P_2 P_3 P_4}{n_1 n_2 n_3} \right).$$

Table 2 shows the contribution of the terms in the paraxial power equation (5) of the tear-film–cornea reference model of Table 1. The power contributions from previous single-layer models (Liou and Brennan model[21] and Navarro model[22]) are also computed for comparison.

Table 2. Paraxial Power Contributions (D) of the Terms in Eq. (5) in the Different Models

Model	P_1	P_2	P_3	P_4	T_1	T_2	T_3	T_g
Gradient stroma	42.8208	8.1321	−2.7487	−5.7812	0.0001	0.0167	0.0694	9e−6
Homogeneous stroma	42.8208	8.1321	−3.2068	−6.3281	0.0002	0.0186	0.1038	1.2e−5
Liou model	48.3912	0	0	−6.2500	0.1209	0	0	0
Navarro model	48.7047	0	0	−5.9385	0.1156	0	0	0

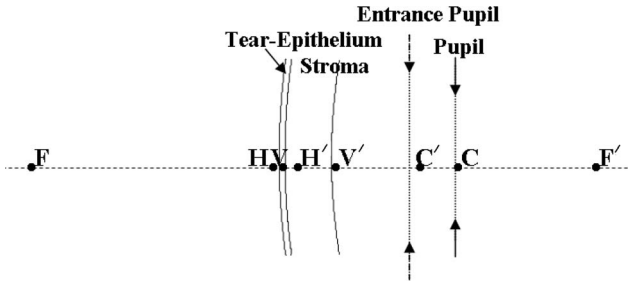

Fig. 2. Cardinal points for the tear–cornea model. Distances from the left to the right are positive sign. F and F′, focal points; H and H′, principal points; V and V′, anterior and posterior vertex of the tear–cornea, respectively; C, location of the physical pupil; C′, location of the entrance pupil. If V′C is set to be 3.5 mm, VF=23.5659 mm, V′F′=30.9858 mm, HF=−23.5243 mm, H′F′=31.4285 mm, VH=−0.0416 mm, V′H′ =−0.4427 mm.

It is important to remark that the total power in the homogeneous-stroma model is 41.541 D, while in the gradient-stroma model it is 42.509 D. Moreover, the total paraxial powers of the cornea in Liou's and Navarro's models, 42.262 D and 42.882 D, respectively, are closer to the gradient model, supporting the importance of the gradient stroma in the multilayer model.

D. Entrance Pupil of the Tear-Film–Cornea Model: Cardinal Points

An immediate application of the ray-transfer matrix of the tear-film–cornea model is to evaluate its cardinal points and from them the entrance pupil location and magnification; I will need this information to evaluate the spherical aberration in Section 5. It is straightforward to find expressions that relate the cardinal points and the paraxial coefficients [see, e.g., Eqs. (22)–(25) and (33)–(36) in Ref. 23]. Figure 2 shows the cardinal points in the tear-film–cornea model. V and V′ are the anterior and posterior vertex points of the tear film and cornea, respectively. H and H′ are the principal points, F and F′ the focal points. C is the location of the physiological pupil. For a generic distance V′C=3.5 mm the magnification of the entrance pupil is 1.1434 and the distance from the posterior vertex of the cornea to the entrance pupil is V′C′ =2.9317.

5. SPHERICAL ABERRATION

A. Primary Spherical Aberration

I consider only primary spherical aberration (neglecting higher-order terms). From the addition theorem[13] in aberration theory, the aberration coefficients of the whole system can be evaluated as the sum of the corresponding coefficients associated with the individual elements. For surface contributions, I use here the notation and derivation of the primary spherical aberration as done by Schwarzschild (see Born and Wolf[13]):

$$W_{40} = \frac{1}{8}\sum_i h_i \left[\frac{Q_i}{R_i^3}(n_i - n_{i-1}) + \left(n_{i-1}\left(\frac{1}{R_i} - \frac{1}{s_i} \right) \right)^2 \times \left(\frac{1}{n_i s_i'} - \frac{1}{n_{i-1} s_i} \right) \right]. \quad (6)$$

Here R_i is the apical radius of the interface surface, Q_i is the asphericity, n_i and n_{i-1} are the refractive indices after and before the interface, respectively, s_i and s_i' are the distances to the surface vertex of the object and image point, and h_i is a parameter depending on the incidence height of the ray on the surface. s_i, s_i', and h_i are evaluated with the recurrent paraxial formulas [e.g., Eqs. (14)–(16) in Subsection 5.5.1 of Ref. 13]. The transverse-ray aberration coefficient σ_1 [needed for Eq. (1)] is obtained from the wave aberration and the distance from the last surface to the image paraxial plane[13]:

$$\sigma_1 = 4W_{40}(s_i'/n_i). \quad (7)$$

B. Transfer Contribution of the Gradient Stroma to the Spherical Aberration

The transfer of rays inside an axial gradient structure introduces spherical aberration. This was studied by among others, Sands, who derived expressions for primary spherical aberration in axial gradients.[24] However, such formulas are quite complex. Fortunately, when the variation of the refractive index is weak, it is possible to derive a simpler formula. Here I follow Wang and Moore.[25] Formally, the weak condition imposes that the incoming Y coordinate of a ray be much bigger than the output ray angle U. In the case of the stroma, the ratio between the two magnitudes is 31, which justifies the weak formulation:

$$\sigma_1 = -\Delta n h_i(h_i/s_i'). \quad (8)$$

Here Δn is the difference in refractive index between the posterior and the anterior part of the stroma.

Table 3 shows the surface and stroma transfer contributions to the wave primary spherical aberration (W_{40}) in the homogeneous and gradient models and, for comparison, in Liou[21] and Navarro's[22] schematic models.

6. APPLICATIONS

An important application of the new equations is that they can be used in different clinical situations to estimate changes in refractive powers where some knowledge of the change of the optical parameters in the cornea and tear film are known *a priori*. Now I present an example in orthokeratology. Orthokeratology is an ophthalmic technique based on the application of contact lenses to modify the shape of the cornea. The refraction changes generated with this technique are classically explained simply by assuming an overall bending model of the cornea. However, new hypotheses have recently been formulated to explain the refraction changes with orthokeratology. Alharbi and Swarbrick[26] suggested that the redistribution of corneal tissue, especially epithelial tissue, could play an important role in refraction changes (in orthokeratology reverse-geometry lens design). They measured the changes in the central and periphery thickness of the stroma and epithelium after 90 days of treatment in 18 subjects for whom a correction of 2.63 ± 0.67 D was achieved.

Using their experimental data, I derived a model for the cornea before and after treatment (see Table 4), where I kept constant the refractive indices and the shape of the

first interface (air–tear film) with the purpose of evaluating just the contribution to the refraction of the corneal tissue redistribution. With such a model it is easy to prove that the change in paraxial optical power is 0.36 D, whereas refraction change measured clinically is 2.63 D. This result suggests that the contribution of corneal tissue redistribution to power changes is relatively small. Flattening of the tear-film–epithelial surface and/or possibly some change in the refractive indices could play the main role in power changes with orthokeratology.

7. DISCUSSION

I have derived the formulas to calculate the paraxial focal length and plane of best focus of a multilayer model of the human cornea and tear film. The usefulness of such formulas lies in the straightforward analysis of the role of the different parameters of the tear-film–cornea model to its optical power. I examine these roles using the reference model of Table 1. Table 2 gives the contributions of the different surfaces to the paraxial power. As expected, the major contribution is the air–tear-film-surface contribution. However the other surfaces contribute significantly to the total power. Moreover, the consideration of a stroma with an axial index of refraction distribution implies a reduction in the refractive index changes in the stroma interfaces (see Fig. 1) and therefore a less negative power contribution of these interfaces (see Table 2). It should be noted that the smoothing of the interface refractive change due to the gradient structure of the stroma creates a natural gradient-index reflection-reduction property compared with the case of a homogeneous stroma.

The spherical aberration of the multilayer model has also been analyzed in comparison with previous schematic models. Figure 3 shows the changes of spherical aberration with the pupil size radius in the multilayer gradient-stroma model in comparison with Liou's[21] and Navarro's[22] models. The higher ratio of the increase of spherical aberration to pupil size in the multilayer model again reveals the role of the gradient index of the stroma.

It is also interesting to evaluate the change in the plane of best focus with the position of the object in the optical axis. Figure 4 shows how the plane of best focus changes between typical near points (20 cm) to far points (10 m). An interesting result is that the difference between plane of best focus in the gradient and the homogeneous model tends to decrease for near points. This oc-

Table 3. Wave Primary Spherical Aberration (W_{40}) Contributions (mm^{-3})

Models	Air–Tear	Tear–Epithelium	Epithelium–Stroma	Stroma–Aqueous	Stroma Transfer	Total
Gradient stroma	3.280×10^{-5}	0.109×10^{-5}	0.765×10^{-5}	0.055×10^{-5}	0.242×10^{-5}	4.450×10^{-5}
Homogeneous stroma	3.280×10^{-5}	0.109×10^{-5}	0.873×10^{-5}	0.051×10^{-5}	0	4.310×10^{-5}
Liou model	3.490×10^{-5}	0	0	0.45×10^{-5}	0	3.940×10^{-5}
Navarro model	2.740×10^{-5}	0	0	-0.541×10^{-5}	0	2.200×10^{-5}

Table 4. Parameters of the Cornea Multilayer Model before and after Orthokeratology Treatment Considering Only Corneal Tissue Redistribution

	Interface			
	Air–Tear	Tear–Epithelium	Epithelium–Stroma	Stroma–Aqueous
Before Orthokeratology Treatment				
Radius	7.8700	7.8700	7.8387	7.5185
Q	−0.1800	−0.1800	−0.2310	−0.1647
	Medium			
	Tear	Epithelium	Stroma	Aqueous
Central thickness	0.0040	0.0499	0.5431	—
After 90 Days of Orthokeratology Treatment				
	Interface			
Radius	7.8700	7.8700	7.5769	7.1326
Q	−0.1800	−0.1800	−0.4533	−0.522
	Medium			
	Tear	Epithelium	Stroma	Aqueous
Central thickness	0.0040	0.0309	0.5431	—

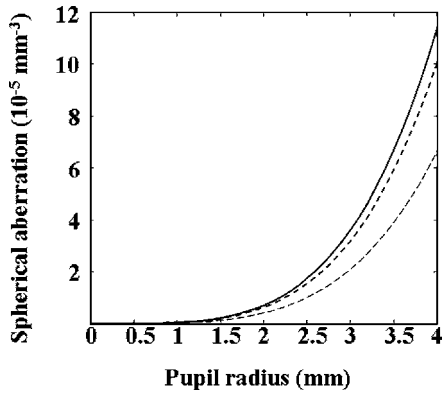

Fig. 3. Spherical aberration coefficient W_{40} versus pupil radius (in millimeters) in the gradient multilayer model (solid curve), Liou's model (short-dashed curve) and Navarro's model (long-dashed curve).

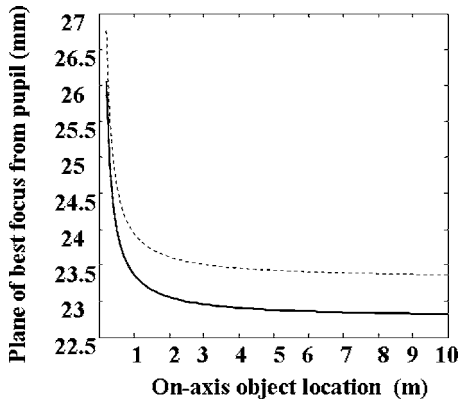

Fig. 4. Plane of best focus (in millimeters) with respect to the exit pupil versus on-axis object position with respect to tear anterior vertex. The solid curve shows the gradient and the dashed curve the homogeneous stroma model.

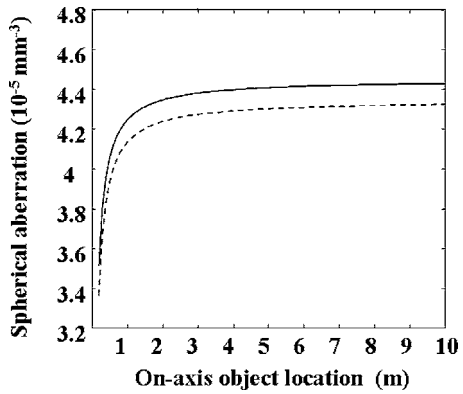

Fig. 5. Spherical aberration coefficient W_{40} versus on-axis object position with respect to the cornea. The solid curve shows the gradient and the dashed curve the homogeneous stroma model.

curs because the stroma axial transfer contribution to the spherical aberration becomes smaller for nearer objects (Fig. 5).

The importance of considering gradient structures in the human eye, specifically in the crystalline lens, has a long tradition in visual optics, from the classical works of Gullstrand[27] to more recent works; see, e.g., Ref. 28 and references therein.

The great potential of the present work lies in studying situations where the internal structure of the cornea and tear film are modified, as shown in a practical example in Section 6. The author is now preparing a continuing work where some other examples will be studied in more detail: changes in the power with epithelial distortion, cornea swelling, and corneal refractive surgery.

As a final remark, it should be considered that this analysis could be extended to the whole eye, including the crystalline lens. In fact, an analysis of the paraxial properties of the crystalline lens has been done recently by Perez *et al.*[23]

The code used in this paper (written in MATLAB) is available from the author.

APPENDIX A: DERIVATION OF THE PARAXIAL COEFFICIENTS FOR AN AXIAL LINEAR GRADIENT INDEX

The stationary action principle in geometrical optics is expressed in a variational equation:

$$\delta \int N(r)\mathrm{d}s = 0, \tag{A1}$$

where $N(r)$ is the refractive index function of spatial coordinates and ds is the differential line segment of the ray trajectory. When the system is rotationally symmetric with respect to the z axis, ds can be written as

$$\mathrm{d}s = (\mathrm{d}Y^2 + \mathrm{d}z^2)^{1/2} = \mathrm{d}z\left(\frac{\mathrm{d}Y^2}{\mathrm{d}z^2} + 1\right)^{1/2}, \tag{A2}$$

where Y is expressed as a function of z (physically meaning that the rays do not reverse their trajectory on the z axis). Thus, we can rewrite Eq. (A1) as

$$\delta \int N(Y,z)(1 + Y'^2)^{1/2}\mathrm{d}z = \delta \int \mathcal{L}(Y,Y',z)\mathrm{d}z = 0, \tag{A3}$$

where the prime denotes the differential with respect to z and $\mathcal{L}$ is the Lagrangian, which depends on three variables: Y, Y', and z. A necessary condition for the variational equation (A3) is stated by the Euler–Lagrange differential equation.[29] $\mathcal{L}$, considered a function of three independent variables, must satisfy

$$\frac{\partial \mathcal{L}(Y,Y',z)}{\partial Y} - \frac{\mathrm{d}}{\mathrm{d}z}\left[\frac{\partial \mathcal{L}(Y,Y',z)}{\partial Y'}\right] = 0. \tag{A4}$$

In an axial gradient, N depends only on z [$N(z)$]. Thus the Lagrangian depends only on Y' and z [$L(Y',z)$]:

$$\frac{\mathrm{d}}{\mathrm{d}z}\left\{N(z)\frac{\partial[(1 + Y'^2)^{1/2}]}{\partial Y'}\right\} = \frac{\mathrm{d}}{\mathrm{d}z}\left\{N(z)\frac{Y'}{(1 + Y'^2)^{1/2}}\right\} = 0. \tag{A5}$$

Equation (A5) is the general differential equation for axial gradients. In the paraxial approximation of Eq. (A5), Y' (the angle tangent of the ray with the z axis) is very small, $Y' \ll 1$:

$$\frac{\mathrm{d}}{\mathrm{d}z}(N(z)Y') = 0. \tag{A6}$$

In other words, the product NY' is invariant with z:

$$Y'(z) = \frac{N(0)Y'(0)}{N(z)}. \tag{A7}$$

Integrating Eq. (A7),

$$\int_0^t Y'(z)\mathrm{d}z = Y(z) - Y(0) = N(0)Y'(0)\int_0^t \frac{\mathrm{d}z}{N(z)}, \tag{A8}$$

where t is the propagation distance in the z axis. For a linear gradient, $N(z)=N_a+(N_p-N_a/t)z$, the integral of Eq. (A8) can be easily computed:

$$Y(z) = Y(0) + N_a Y'(0)\frac{t\,\ln(N(z)/N_a)}{(N_p - N_a)}. \tag{A9}$$

Finally, from Eqs. (A7)–(A9) we get the paraxial coefficients:

$$A = 1, \qquad B = \frac{tN_a \ln(N(z)/N_a)}{(N_p - N_a)}, \qquad C = 0, \qquad D = \frac{N(0)}{N(z)}. \tag{A10}$$

ACKNOWLEDGMENTS

I thank Arthur Bradley and Sowmya Ravikumar for their valuable comments and suggestions. This work has been done with funding from Ministerio de Educación y Ciencia (Spain) through a Fulbright postdoctoral fellowship.

Sergio Barbero's e-mail address is sergio.barbero@io.cfmac.csic.es.

REFERENCES

1. D. A. Atchison and G. Smith, *Optics of the Human Eye* (Butterworth-Heinemann, 2000).
2. J. M. Schmitt and G. Kumar, "Turbulent nature of refractive-index variations in biological tissue," Opt. Lett. **21**, 1310–1312 (1996).
3. D. R. Korb, *The Tear Film: Structure, Function, and Clinical Examination* (Butterworth-Heinemann, Oxford, 2002).
4. J. P. Craig, P. A. Simmons, S. Patel, and A. Tomlinson, "Refractive-index and osmolality of human tears," Optom. Vision Sci. **72**, 718–724 (1995).
5. S. Patel, D. Z. Reinstein, R. H. Silverman, and D. J. Coleman, "The shape of Bowman's layer in the human cornea," J. Refract. Surg. **14**, 636–640 (1998).
6. G. Smolin and R. A. Thoft, *The Cornea: Scientific Foundations and Clinical Practice* (Little, Brown, 1994).
7. S. Patel, J. Marshall, and F. W. Fitzke, "Refractive-index of the human corneal epithelium and stroma," J. Refract. Surg. **11**, 100–105 (1995).
8. C. W. Oyster, *The Human Eye: Structure and Function* (Sinauer, 1999).
9. D. M. Maurice, "The structure and transparency of the cornea," J. Physiol. **136**, 263–286 (1957).
10. M. Dubbelman, H. A. Weeber, R. G. L. van der Heijde, and H. J. Volker-Dieben, "Radius and asphericity of the posterior corneal surface determined by corrected Scheimpflug photography," Acta Ophthalmol. Scand. **80**, 379–383 (2002).
11. M. P. Keating, *Geometric, Physical, and Visual Optics* (Butterworth-Heinemann, 2002).
12. X. Cheng, A. Bradley, and L. N. Thibos, "Predicting subjective judgment of best focus with objective image quality metrics," J. Math. Imaging Vision **4**, 310–321 (2004).
13. M. Born and E. Wolf, *Principles of Optics: Electromagnetic Theory of Propagation, Interference and Diffraction of Light* (Pergamon, 1980).
14. K. Miyamoto, "Image evaluation by spot diagram using a computer," Appl. Opt. **2**, 1247–1250 (1963).
15. P. J. Sands, "Aberration coefficients and surfaces of best focus," J. Opt. Soc. Am. **63**, 582–590 (1973).
16. D. A. Atchison and G. Smith, "Chromatic dispersions of the ocular media of human eyes," J. Opt. Soc. Am. A **22**, 29–37 (2005).
17. R. K. Luneburg, *Mathematical Theory of Optics* (University of California Press, Berkeley, 1964).
18. H. A. Buchdahl, *Optical Aberration Coefficients* (Dover, New York, 1968).
19. F. J. Dijksterhuis, *Lenses and Waves: Christiaan Huygens and the Mathematical Science of Optics in the Seventeenth Century*, Vol. 9 of Archimedes Series (Springer, 2004).
20. P. J. Sands, "Inhomogeneus lenses III. Paraxial optics," J. Opt. Soc. Am. **61**, 879–885 (1971).
21. H. L. Liou and N. A. Brennan, "Anatomically accurate, finite model eye for optical modeling," J. Opt. Soc. Am. A **14**, 1684–1695 (1997).
22. R. Navarro and J. Santamaria, "Accommodation dependent model of the human eye with aspherics," J. Opt. Soc. Am. A **2**, 1273–1281 (1985).
23. M. V. Pérez, C. Bao, M. T. Flores-Arias, M. A. Rama, and C. Gómez-Reino, "Description of gradient-index crystalline lens by a first-order optical system," J. Opt. A, Pure Appl. Opt. **1**, 103–110 (2005).
24. P. J. Sands, "Third-order aberrations of inhomogeneous lenses," J. Opt. Soc. Am. **60**, 1436–1443 (1970).
25. D. Y. Wang and D. T. Moore, "Third-order aberration theory For weak gradient-index lenses," Appl. Opt. **29**, 4016–4025 (1990).
26. A. Alharbi and H. A. Swarbrick, "The effects of overnight orthokeratology lens wear on corneal thickness," Invest. Ophthalmol. Visual Sci. **44**, 2518–2523 (2003).
27. H. Helmholtz, *Helmholtz's Treatise on Physiological Optics* (Optical Society of America, 1924).
28. G. Smith, "The optical properties of the crystalline lens and their significance," Clin. Exp. Optom. **86**, 3–18 (2003).
29. M. Kline, *Mathematical Thought from Ancient to Modern Times* (Oxford U. Press, 1972).